The Journal of Physical Chemistry Letters

Letter

Enhanced Electrical Properties and Air Stability of Amorphous Organic Thin Films by Engineering Film Density

Yu Esaki, Takeshi Komino, Toshinori Matsushima, and Chihaya Adachi

J. Phys. Chem. Lett., **Just Accepted Manuscript** • DOI: 10.1021/acs.jpclett.7b02808 • Publication Date (Web): 15 Nov 2017

ACS Publications

The Journal of Physical Chemistry Letters is published by the American Chemical Society. 1155 Sixteenth Street N.W., Washington, DC 20036

Enhanced Electrical Properties and Air Stability of Amorphous Organic Thin Films by Engineering Film Density

Yu Esaki,[1,2] Takeshi Komino,[1-3] Toshinori Matsushima,[1,2,4] and Chihaya Adachi[*,1-4]*

[1]Center for Organic Photonics and Electronics Research (OPERA), Kyushu University, 744 Motooka, Nishi, Fukuoka 819-0395, Japan

[2]Japan Science and Technology Agency (JST), ERATO, Adachi Molecular Exciton Engineering Project, 744 Motooka, Nishi, Fukuoka 819-0395, Japan

[3]Education Center for Global Leaders in Molecular System for Devices, Kyushu University, 744 Motooka, Nishi, Fukuoka 819-0395, Japan

[4]International Institute for Carbon Neutral Energy Research (WPI-I^{2}CNER), Kyushu University, 744 Motooka, Nishi, Fukuoka 819-0395, Japan

Corresponding Author
Chihaya Adachi

E-mail: adachi@cstf.kyushu-u.ac.jp

Tel: +81-92-802-6920

Fax: +81-92-802-6921

Abstract

The influences of film density and molecular orientation on the carrier conduction and air stability of vacuum-deposited amorphous organic films of *N*,*N*'-di(1-naphthyl)-*N*,*N*'-diphenyl-(1,1'-biphenyl)-4,4'-diamine (*α*-NPD) were investigated. The substrate temperature (T_{sub}) during vacuum deposition had different effects on the film density and molecular orientation of *α*-NPD. Film density was a concave function of T_{sub}; maximum density was attained at T_{sub} = 270–300 K. *α*-NPD molecules were randomly oriented at T_{sub} = 342 K, and their horizontal orientation on the substrate became dominant as T_{sub} decreased. Hole current and air stability were clearly raised by increasing the film density by 1%–2%; these effects were respectively attributed to enhanced carrier hopping between neighboring *α*-NPD molecules and suppressed penetration of oxygen and water. These results imply that increasing film density is more effective to enhance the electrical performance of organic thin-film devices with *α*-NPD films than control of molecular orientation.

TOC

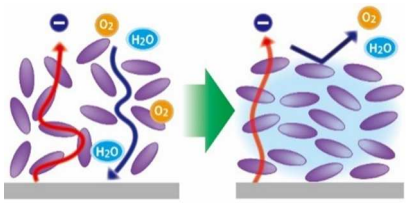

Organic optoelectronic devices such as organic light-emitting diodes (OLEDs), organic solar cells (OSCs), and organic field-effect transistors (OFETs) have attracted wide attention because of their huge potential in future post-inorganic devices by taking advantage of their unlimited molecule design. Organic thin films used in such functional devices can be roughly categorized into polycrystalline and amorphous films. OFETs and OSCs mainly use polycrystalline films because of their high carrier mobilities and long exciton diffusion lengths. However, polycrystalline films constructed of tiny crystals always contain many grain boundaries between the crystals and underlying electrodes. Meanwhile, OLEDs often contain amorphous films, which are smooth and without pinholes, to suppress leakage current. The presence of gaps at grain boundaries in polycrystalline films and gaps originating from inefficient molecular packing in amorphous films strongly limit charge-carrier injection and transport[1−3] and allow oxygen and water molecules to penetrate into organic films, causing the fundamental current–voltage properties and air stability of organic devices to deteriorate.[4−6] Some researchers have suggested that increasing the density of amorphous organic films results in lower moisture penetration.[7,8] Therefore, it is expected that tighter packing of molecules to decrease the gaps in films will improve both their electrical properties and air stability.

Recently, we demonstrated that cold isostatic pressing increases the density and enhances the electrical properties of polycrystalline films by physically compressing the gaps between grain boundaries.[9,10] However, it was virtually impossible to compress amorphous organic films and improve their electrical properties using this method.[10] Thus, we considered an alternative method to densify amorphous films. In this study, we focus our attention on controlling the substrate temperature (T_{sub}) during vacuum deposition of amorphous organic films. Ediger's group has established that controlling T_{sub} during vacuum deposition can produce thermally

stable amorphous films with high film density and molecular anisotropy.[11−15] This is because T_{sub} governs the kinetic mobility of molecules migrating on a film surface during deposition, which strongly affects resulting film morphologies.[11−15] Although kinetic mobility can be affected by other factors, such as deposition rates[12] and substrate roughness,[16] T_{sub} is the most effective, simplest factor to modulate kinetic mobility. Accordingly, it is expected that if highly densified amorphous films can be obtained by controlling T_{sub} during deposition, these films should display enhanced electrical properties and air stability. In this study, we comprehensively investigate the influence of T_{sub} on the film density, molecular orientation, electrical properties, and air stability of amorphous *N*,*N*'-di(1-naphthyl)-*N*,*N*'-diphenyl-(1,1'-biphenyl)-4,4'-diamine (α-NPD) films. It is revealed that an increase of film density achieved by controlling T_{sub} simultaneously leads to enhanced electrical properties and air stability. Although T_{sub} also controls the molecular orientation, molecular orientation has less influence than density on electrical properties and air stability of the α-NPD films.

We used α-NPD, whose chemical structure is shown in the inset of Fig. 1(c), to fabricate films and devices because it is widely known to form amorphous films by vacuum deposition.[17] For the measurements of density and molecular orientation, α-NPD films with a thickness of approximately 100 nm were vacuum-deposited on silicon substrates kept at various T_{sub} ranging from 212 to 342 K. α-NPD films obtained at these T_{sub} were in the amorphous state and had very smooth surfaces without pinholes. In contrast, α-NPD films fabricated at T_{sub} = 200 K were opaque and had large surface roughness. We speculate that water molecules condensed in the films during α-NPD deposition at this T_{sub} (around 200 K) and then evaporated from films when T_{sub} was increased to room temperature after α-NPD deposition, which may result in the rough surface. Variable angle spectroscopic ellipsometry (VASE) was performed on the vacuum-

deposited α-NPD films on Si substrates to evaluate their molecular orientation, refractive index n, extinction coefficient k, and film thickness d. As we discuss later, the molecular orientation evaluated by VASE measurement changed markedly depending on T_{sub}, corresponding to a change of the transition dipole orientation in the films. The transition dipole moment of α-NPD is known to be parallel to its long molecular axis.[18] The n and k spectra of organic semiconductor films are known to show anisotropy between the directions parallel and perpendicular to the substrate plane because of the orientation of molecules, even in amorphous films.[13–16,18–21] VASE results were analyzed with an optical model to simultaneously obtain d values and n and k spectra (see Table S1 and S2 and Fig. S1, S2, and S3 in the Supporting Information for the detailed analysis). The molecular orientation in each α-NPD film was evaluated by calculating the orientational order parameter (S), which is defined as:[16,20]

$$S = \frac{k_z - k_x}{k_z + 2k_x}, \quad (1)$$

where k_x and k_z are the extinction coefficients in the directions parallel and perpendicular to the substrate, respectively. The relative density (ρ_{rel}) of each α-NPD film was estimated from the ratio of d values before and after annealing at a temperature higher than the glass transition temperature ($T_{g,\,bulk}$) of α-NPD. The annealing process resulted in the formation of randomized molecular films with a certain density, the value of which is generally lower than that of as-deposited films, as reported previously.[13,18,21]

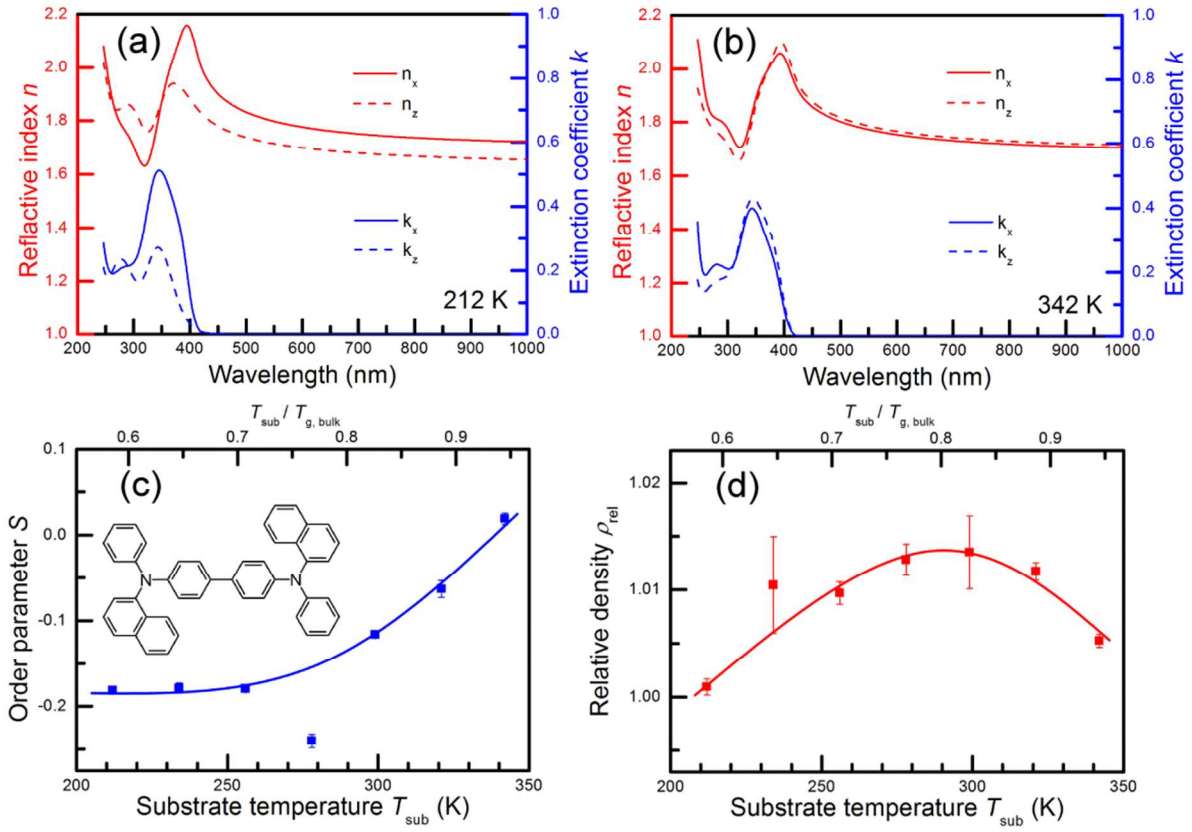

Fig. 1. Refractive index n and extinction coefficient k spectra of representative α-NPD films vacuum-deposited on substrates kept at (a) 212 and (b) 342 K. Plots of (c) orientational order parameter S and (d) relative density ρ_{rel} as a function of substrate temperature during vacuum deposition T_{sub}. The chemical structure of α-NPD is shown in the inset of (c).

Figure 1(a) and (b) display the n and k spectra of α-NPD films vacuum-deposited at T_{sub} = 212 and 342 K. While n_x and k_x were similar to n_z and k_z for films vacuum-deposited at T_{sub} = 342 K, anisotropy of both n and k began to appear and became larger at low T_{sub} (see Fig. S4 in the Supporting Information for the n and k spectra of α-NPD films vacuum-deposited at other substrate temperatures). The large anisotropy of the n and k spectra can be attributed to the anisotropy of the molecular orientation of α-NPD.[13–16,18–21]

The S values estimated from the spectra at a wavelength of 344 nm using Eq. (1) are plotted as a function of T_{sub} in Fig. 1(c). Molecules (transition dipole moments) are vertically oriented, random, and horizontally oriented at S values of 1, 0, and −0.5, respectively. Therefore, the S value of nearly 0 for films vacuum-deposited at T_{sub} = 342 K indicates the randomization of α-NPD molecules. The S value decreased as T_{sub} was lowered, indicating a gradual change from no orientational order to the horizontal orientation of α-NPD molecules. Below this T_{sub}, the S values became almost constant. Similar T_{sub}-dependent orientations have been observed for other organic films.[13−15]

The ρ_{rel} values calculated for films fabricated at each T_{sub} from the change of d are plotted against T_{sub} in Fig. 1(d). No obvious crystallization was observed in all samples. We found that ρ_{rel} was a concave function of T_{sub} and the maximum ρ_{rel} was observed between 270 and 300 K (0.75−0.83 $T_{g, bulk}$), which is close to that previously reported.[13] At low T_{sub}, the kinetic mobility of molecules at a substrate surface is low, so molecules can move only a short distance and have difficulty finding an energetically stable position, leading to smaller ρ_{rel}. In contrast, at high T_{sub}, α-NPD molecules have sufficient kinetic mobility (a long enough molecular movement distance) to reach a more stable position, thereby resulting in higher ρ_{rel}. When T_{sub} was higher than about 0.8 $T_{g, bulk}$, ρ_{rel} decreased again. This would be because the excess kinetic mobility makes it difficult to keep molecules at a stable position. Thus, to obtain the highest ρ_{rel}, a substrate needs to be kept at about 0.8 $T_{g, bulk}$ during vacuum deposition of α-NPD films.

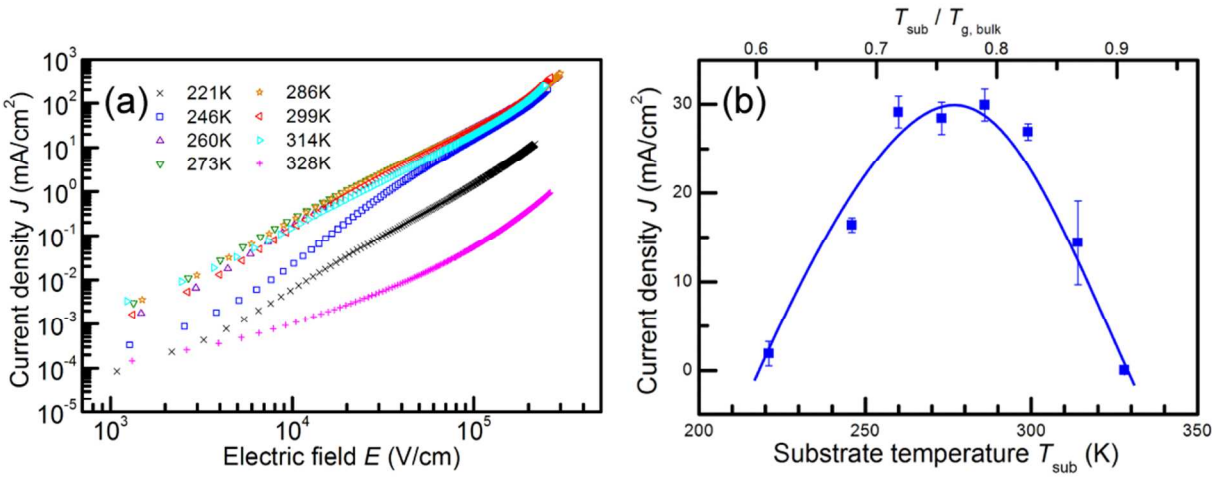

Fig. 2. (a) Representative current density (J)–electric field (E) properties of hole-only devices with α-NPD layers vacuum-deposited at different substrate temperatures (T_{sub}) and (b) a plot of J at $E = 1.0 \times 10^5$ V/cm versus T_{sub}.

We now examine how T_{sub} affects the electrical properties and air stability of α-NPD films considering the variations of S and ρ_{rel}. For this purpose, hole-only devices (HODs) containing an α-NPD layer were fabricated. The structure of the HODs was glass substrate/indium tin oxide (ITO) anode (100 nm)/α-NPD (about 350 nm)/MoO_3 (30 nm)/Au cathode (50 nm). The α-NPD layer was vacuum-deposited at different T_{sub} and the MoO_3 and Au layers were vacuum-deposited on room-temperature substrates. We used MoO_3/Au as the cathode in the HODs because these layers are expected to be more stable in air than the Al and MgAg cathodes commonly used in OLEDs. Because of the high work functions of MoO_3 and Au, electron injection was completely prevented in this structure. Figure 2(a) shows the current density (J)–electric field (E) properties of the HODs. It is clear that the J-E properties are strongly affected by T_{sub}. Below about 3.0×10^4 V/cm, we observed a bend in the J-E properties for all of the devices except for those with α-NPD layers fabricated at T_{sub} = 314 and 328 K. Although the

reason for the bend is still unclear and is under investigation, we tentatively attribute this to an increase of carrier trap density or variation of the energy levels involved in hole transport. The J values at an E of 1.0×10^5 V/cm without the influence of the bend are plotted as a function of T_{sub} in Fig. 2(b). J changes in a similar manner to that of ρ_{rel} in Fig. 1(d). T_{sub} where the maximum J was obtained was 260–290 K (0.72–0.80 $T_{g, bulk}$), which is not far from the results for ρ_{rel} [270–300 K (0.75–0.83 $T_{g, bulk}$)]. A higher ρ_{rel} indicates decreased intermolecular distance because the α-NPD molecules are packed more closely, which might be expected to enhance carrier transport in a film. In contrast, there was no clear relationship between J and S, even though it has been reported that the horizontal orientation on a substrate leads to enhanced carrier transport because of the better overlap of π orbitals between neighboring molecules in a substrate normal. There is a possibility that the density and orientation are different between films vacuum-deposited on ITO-coated glass substrates and Si substrates even at the same T_{sub} because of different substrate surface roughness.[16] Also, the molecular orientation might be different between the film surface and interior, which can change the energy level.[22] However, the substrate-dependent density and orientation and orientation-dependent energy level did not appear to be major factors in our samples because J was strongly related to ρ_{rel} and not S. We note that the ρ_{rel} and S values estimated by VASE here are the average values of the whole films. From the above results, we conclude that for α-NPD, the film density has more influence on carrier transport than the molecular orientation does. Even though the ρ_{rel} variation observed here is very small, just 1%–2%, the effect of ρ_{rel} on J is considerable, as illustrated in Fig. 2(b).

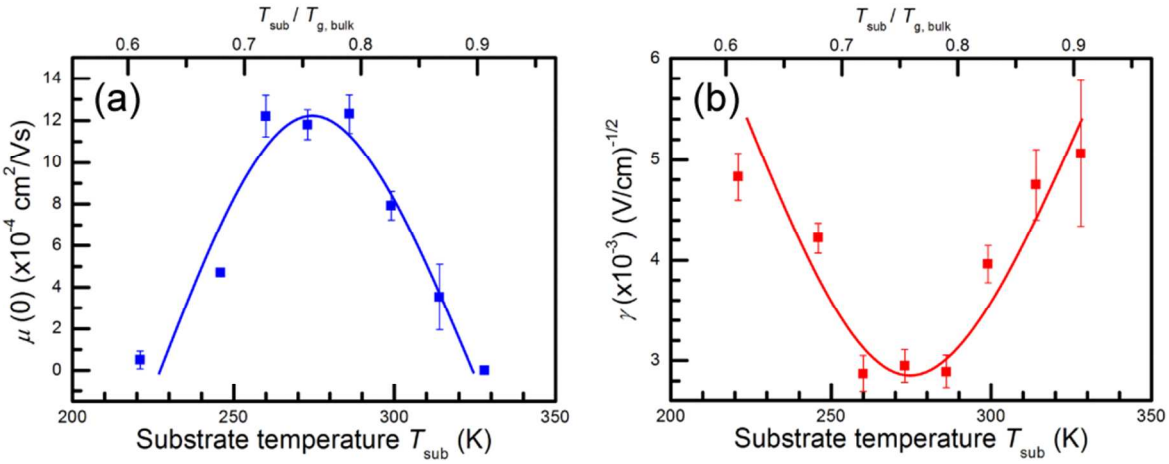

Fig. 3. Plots of (a) zero field mobility $\mu(0)$ and (b) Poole–Frenkel factor γ as a function of T_{sub}. The $\mu(0)$ and γ values were obtained by fitting the *J-E* properties in Fig. 2(a) with Eq. (2).

To gain insight into the observed increase of *J*, the *J-E* curves were analyzed with an injection-limited current (ILC) model, which can be given by:[23–25]

$$J = 4N_0\psi^2 eE exp(-e\phi_B/k_BT)\exp(f^{0.5})\mu(0)\exp(\gamma E^{0.5}), \quad (2)$$

where N_0 is the density of chargeable sites in an organic film, e is the elementary charge, ϕ_B is the injection barrier height, k_B is the Boltzmann constant, T is the temperature, $\mu(0)$ is the zero-field carrier mobility, γ is the Poole–Frenkel factor, f is the reduced electric field ($f = e^3E/4\pi\varepsilon_0\varepsilon_r{k_B}^2T^2$), ε_0 is the vacuum permittivity, ε_r is the relative permittivity, and ψ is a function of f [$\psi = f^{-1} + f^{-0.5} - f^{-1}(1 + 2f^{0.5})^{0.5}$]. Fitting was performed with $\mu(0)$ and γ as variables in the high voltage region, where the influence of the bend seems negligible (see the Experimental Methods for the fitting details and Fig. S5 in the Supporting Information for the fitting results). Figure 3(a) and (b) show $\mu(0)$ and γ for which the best fitting results were obtained, respectively. The results reveal that the highest $\mu(0)$ and lowest γ appear at 260–290 K (0.72–0.80 $T_{g, bulk}$), nearly agreeing with the T_{sub} values where the maximum ρ_{rel} was observed [270–300 K (0.75–0.83 $T_{g, bulk}$)]. In films with higher density, the width of their density of states

(DOS) might be expected to be narrower because of the location of molecules at stable positions. This DOS narrowing can result in a lower barrier between neighboring states near the center of the DOS distribution. The changes of tail state and state-to-state barrier caused by the DOS narrowing could lead to a decrease of activation energy and enhanced rate of carrier hopping, which could be the origins of the increased $\mu(0)$ and decreased γ.

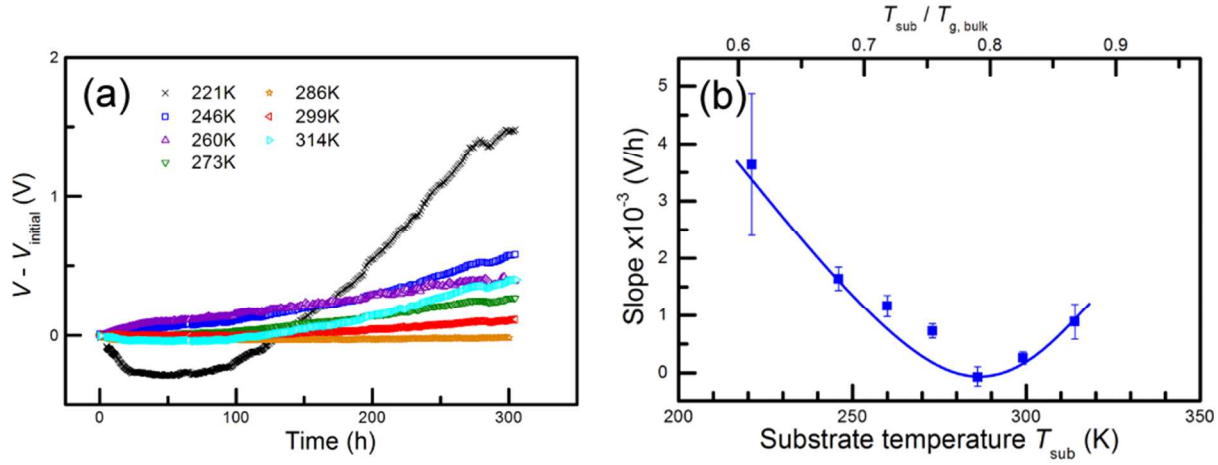

Fig. 4. (a) Temporal changes of V for HODs with α-NPD layers vacuum-deposited at different T_{sub}. To obtain these data, HODs were operated at a fixed current density of 0.1 mA/cm^2 in air under dark conditions. To make it easier to compare the changes of V, the initial V at 0 min was offset to 0 V. To quantitatively evaluate air stability, slopes were calculated by dividing the difference in V between 0 and 300 h by the elapsed time (300 h). The calculated slopes are shown in (b).

After measurement of the initial J-E properties, the air stability of HODs was evaluated from the temporal changes of driving voltage under continuous current application at 0.1 mA/cm^2 in air under dark conditions (Fig. 4(a)). To make it easier to compare the temporal V changes

between different HODs, the initial voltage ($V_{initial}$) at 0 h in Fig. 4(a) was offset to 0 V by subtracting $V_{initial}$ from V. For most of the devices, $V - V_{initial}$ values increased monotonically over time. Devices with α-NPD vacuum-deposited at the lowest T_{sub} of 221 K showed unique behavior; $V - V_{initial}$ values decreased during initial device operation and then began to increase rapidly; the reason for this is still unclear and needs to be investigated. To quantitatively evaluate the air stability of the HODs from Fig. 4(a), slopes were calculated by dividing the difference in $V - V_{initial}$ between 0 and 300 h by the elapsed time of 300 h; the results are displayed in Fig. 4(b). In this figure, a smaller slope means higher air stability. The air stability data matched the ρ_{rel} curve well. These data reveal that α-NPD films with higher ρ_{rel} have higher air stability, while S has no relation to not only the electrical properties but also the air stability of the films. There is a possibility that S changes during the stability measurements. However, such a change of S should not markedly affect the stability results because carrier transport properties did not depend on S for α-NPD, as we discussed earlier.

An increase of V under continuous driving of organic devices may be caused by several factors including (1) degradation of metal electrodes,[26] (2) decomposition of organic materials via excited states,[27] (3) crystallization of amorphous films,[6] and (4) absorption of gas molecules by films.[4–8,28] Factor (1) can be ruled out here because the ITO, Au, and MoO_3 layers should be relatively stable in air and were used in all of the devices discussed here. Also, factor (2) can be ignored because no excited state is formed by carrier recombination in our HODs.[27] It is expected that crystallization during device operation is likely suppressed for thermally stable films with high density. Optical microscopy revealed no marked α-NPD crystallization for all devices after 300 h of continuous driving. Thus, factor (3) is assumed not to be dominant. There are several reports describing film density being related to absorption of gas molecules.[7,8,28]

Results in some reports[7,8] indicated that densification of organic films led to decreased water uptake, consistent with our present results. Conversely, water uptake decreased when T_{sub} was above room temperature, where the film density is expected to be lower, in another study.[28] Thus, how film density affects absorption of gas molecules (water uptake) by films is still unclear. Based on our results discussed earlier, air stability is undoubtedly enhanced with increasing film density. Therefore, we speculate that absorption of water and oxygen by the HODs operating in air is suppressed when the α-NPD film has higher density. Thus, factor (4) is a probable reason for the observed increase in V over time because the inclusion of water and oxygen into organic films accelerates degradation.[4–6] The detailed mechanism of the improved air stability with increased film density will be clarified in the future. In addition, it will be necessary to investigate whether water or oxygen is the main cause of device degradation.

The present study revealed that the horizontal orientation of molecules has little influence on film electrical properties and air stability. However, horizontal orientation is very important to enhance the light outcoupling efficiency of OLEDs.[29,30] If horizontal orientation and high density can be achieved in the same film by controlling the chemical structures of organic materials and T_{sub} during their vacuum deposition, we can realize OLEDs with simultaneous higher external quantum efficiency, lower driving voltage, and higher air stability compared with those of conventional OLEDs. Furthermore, deeper understanding of the aggregation state in amorphous thin films is necessary from a fundamental viewpoint. Our study revealed that increasing the film density by only a few percent greatly improved device physical properties. However, the change in the aggregation state in the films with densification is still not clear. It is conceivable that there is a uniform decrease of intermolecular distance and that the spatial fluctuation of free volume in the films is lowered. We need to conduct thorough investigations to elucidate the relationships

between chemical structures, microscopic amorphous film aggregation, electrical properties, and air stability.

In this study, we investigated the influence of T_{sub} of α-NPD films on their molecular orientation, film density, electrical properties, and air stability. We found that the electrical properties and air stability of the α-NPD films were most enhanced at T_{sub} of around 0.8 $T_{g,bulk}$. The reason for the enhanced electrical properties and air stability is mainly because of an increase of film density at this T_{sub} and not a change of molecular orientation. In OLED fabrication, several kinds of organic layers are generally vacuum-deposited on substrates at room temperature. The results obtained in this study indicate that keeping T_{sub} at 0.8 $T_{g,bulk}$ of materials (slightly lower than room temperature for α-NPD) is very important to achieve the maximum electrical performance and air stability of organic devices.

Experimental Methods

Film fabrication. α-NPD purchased from Nippon Steel & Sumikin Chemical was evaporated under vacuum to fabricate films on bare Si substrates kept at various T_{sub} of 200–350 K under vacuum ($< 1.0 \times 10^{-3}$ Pa). The Si substrates were pre-cleaned by ultrasonication in acetone, detergent, pure water, and isopropanol, followed by UV/O_3 treatment. T_{sub} was calibrated with an alumel/chromel thermocouple attached to the substrate surface after film fabrication. The pressure and deposition rate during the vacuum deposition of α-NPD were of the order of 10^{-4} Pa and 0.13 ± 0.03 nm/s, respectively.

Analysis of film structure. A VASE system (M-2000, J.A. Woollam) was used to evaluate d, n, k, S, and ρ_{rel} of the α-NPD films. In the VASE measurements, the incident light angle ranged from

45° to 75° with a step of 5° and the spectral range was 245–1000 nm. Results from VASE measurements were analyzed by fitting with an anisotropic model using Gaussian-type and Tauc–Lorentz-type oscillators to simultaneously obtain d and spectra of n and k in each axis. For the measurement of ρ_{rel}, α-NPD films were annealed under vacuum (< 1.0×10^{-3} Pa) for 30 min at 381 K after the first VASE measurements, and then cooled to room temperature at a certain rate. This annealing temperature is about 20 K higher than the $T_{g,\,bulk}$ of α-NPD (362 K).[13] The annealed films were measured by VASE again to obtain their d values. VASE evidently indicated the randomization of α-NPD molecules accompanied with the change of optical parameter n and k and a slight increase of d in the annealed films compared with that before annealing. Assuming that the film area and material weight on a substrate were the same before and after annealing, ρ_{rel} values are given by,

$$\rho_{rel} = \frac{d_{annealed}}{d_{as-deposited}}, \quad (3)$$

where $d_{annealed}$ and $d_{as\text{-}deposited}$ are the thicknesses of the annealed and as-deposited films, respectively.

Hole-only device fabrication. The HOD structure used in this study was glass substrate/ITO anode (100 nm)/α-NPD (about 350 nm)/MoO_3 (30 nm)/Au cathode (50 nm). First, glass substrates coated with a 100-nm-thick ITO layer were cleaned as mentioned above. An α-NPD layer with a thickness of about 350 nm was vacuum-deposited on substrates kept at various T_{sub} under the conditions mentioned above. After T_{sub} was returned to room temperature, MoO_3 and Au layers were vacuum-deposited on top of the α-NPD layer to complete the HODs. The active device area was 4 mm^2.

Measurement of electrical properties and air stabilities. *J-V* properties of HODs were measured with a computer-controlled sourcemeter (2400, Keithley) under nitrogen in the dark. We tried to control the *α*-NPD film thickness at 350 nm using a quartz crystal microbalance installed near a substrate in a vacuum chamber. However, actual thicknesses showed slight variation between samples. Therefore, we used *E* instead of *V* to allow better comparison of the film parameters. Here, we calculated *E* used in Fig. 2(a) by simply dividing *V* by the *α*-NPD film thickness of each HOD measured by a profilometer (DEKTAK XT, Bruker). After the *J-V* measurements, the air stability of HODs was evaluated from the temporal change of driving voltage under continuous current application at 0.1 mA/cm^2 in air (without encapsulation) under dark conditions using an OLED lifetime measurement system (EAS-26B, System Engineers Co.). The temperature and relative humidity during the stability measurements were around 24 °C and 50%, respectively.

Estimation of zero-field carrier mobility μ(0) and Poole–Frenkel factor γ. The *J-E* properties were fitted with Eq. (2). Here, N_0 was assumed to be equal to the molecular density of α-NPD in the films and could be obtained by the equation:

$$N_0 = \rho_{abs}\rho_{rel}N_A/\rho_{rel,300K}M_w, \quad (4)$$

where ρ_{abs} is the absolute film density measured at 300 K (1.19 ± 0.01 g/cm^3),[31] ρ_{rel} is the relative film density, $\rho_{abs,300K}$ is the relative film density measured at 300 K, N_A is the Avogadro constant, and M_W is the molecular weight (588.74 g/mol for α-NPD). The standard ε_r value of 3.0 and T of 300 K were used for the ILC analysis. The work function of ITO was 5.0 eV and the ionization energy of α-NPD was 5.4 eV, both of which were measured by photoelectron yield spectroscopy (AC-3, RikenKeiki). Therefore, ϕ_B was estimated to be 0.4 eV. Our HODs had a built-in

potential (V_{bi}), which is probably defined by the difference between the work functions of ITO (5.0 eV) and MoO_3 (5.9 eV, measured by the AC-3 spectrometer). The electric fields of the HODs were calibrated with a V_{bi} value of −0.9 V using the relation: $E_{calibrated} = (V - V_{bi})/d$.

Acknowledgements

This work was supported by JST ERATO Grant Number JPMJER1305, Japan.

Supporting Information

Fitting details of VASE results; the n and k spectra of α-NPD films vacuum-deposited at other substrate temperatures (212, 256, 299, and 342 K); fitting details of the injection-limited current model.

Author Information

ORCID

Yu Esaki: 0000-0002-7575-3707

Notes

The authors declare no competing financial interest.

References

(1) Horowitz, G.; Hajlaoui, M. E. Mobility in Polycrystalline Oligothiophene Field-Effect Transistors Dependent on Grain Size. *Adv. Mater.* **2000**, *12*, 1046–1050.

(2) Kelley, T. W.; Frisbie, C. D. Gate Voltage Dependent Resistance of a Single Organic Semiconductor Grain Boundary. *J. Phys. Chem. B* **2001**, *105*, 4538–4540.

(3) Seki, S.; Terashima, Y.; Kunimi, Y.; Kawamori, T.; Tashiro, M.; Honda, Y.; Tagawa, S. The Effects of Free Volumes on Charge Carrier Transport in Polysilanes Probed by Positron Annihilation. *Radiat. Phys. Chem.* **2003**, *68*, 501–505.

(4) Ikeda, T.; Murata, H.; Kinoshita, Y.; Shike, J.; Ikeda, Y.; Kitano, M. Enhanced Stability of Organic Light-Emitting Devices Fabricated under Ultra-High Vacuum Condition. *Chem. Phys. Lett.* **2006**, *426*, 111–114.

(5) Wölzl, F.; de Moraes, I. R.; Lüssem, B.; Hofmann, S.; Leo, K.; Gather, M. C. Performance and Lifetime of Vacuum Deposited Organic Light-Emitting Diodes: Influence of Residual Gases Present during Device Fabrication. *Org. Electron.* **2014**, *15*, 3251–3258.

(6) Aziz, H.; Popovic, Z.; Xie, S.; Hor, A.-M.; Hu, N.-X.; Tripp, C.; Xu, G. Humidity-Induced Crystallization of Tris (8-Hydroxyquinoline) Aluminum Layers in Organic Light-Emitting Devices. *Appl. Phys. Lett.* **1998**, *72*, 756–758.

(7) Dawson, K. J.; Kearns, K. L.; Ediger, M. D.; Sacchetti, M. J.; Zografi, G. D. Highly Stable Indomethacin Glasses Resist Uptake of Water Vapor. *J. Phys. Chem. B* **2009**, *113*, 2422–2427.

(8) Surana, R.; Pyne, A.; Suryanarayanan, R. Effect of Aging on the Physical Properties of Amorphous Trehalose. *Pharm. Res.* **2004**, *21,* 867–874.

(9) Matsushima, T.; Esaki, Y.; Adachi, C. Enhancement of the Electrical Characteristics of Metal-Free Phthalocyanine Films Using Cold Isostatic Pressing. *Appl. Phys. Lett.* **2014**, *105*, 243301.

(10) Esaki, Y.; Matsushima, T.; Adachi, C. Current Enhancement in Organic Films through Gap Compression by Cold and Hot Isostatic Pressing. *Adv. Funct. Mater.* **2016**, *26*, 2940–2949.

(11) Swallen, S. F.; Kearns, K. L.; Mapes, M. K.; Kim, Y. S.; McMahon, R. J.; Ediger, M. D.; Wu, T.; Yu, L.; Satija, S. Organic Glasses with Exceptional Thermodynamic and Kinetic Stability. *Science* **2007**, *315*, 353–356.

(12) Chua, Y. Z.; Ahrenberg, M.; Tylinski, M.; Ediger, M. D.; Schick, C. How Much Time Is Needed to Form a Kinetically Stable Glass? AC Calorimetric Study of Vapor-Deposited Glasses of Ethylcyclohexane. *J. Chem. Phys.* **2015**, *142*, 054506.

(13) Dalal, S. S.; Walters, D. M.; Lyubimov, I.; de Pablo, J. J.; Ediger, M. D. Tunable Molecular Orientation and Elevated Thermal Stability of Vapor-Deposited Organic Semiconductors. *Proc. Natl. Acad. Sci.* **2015**, *112*, 4227–4232.

(14) Gujral, A.; O'Hara, K. A.; Toney, M. F.; Chabinyc, M. L.; Ediger, M. D. Structural Characterization of Vapor-Deposited Glasses of an Organic Hole Transport Material with X-Ray Scattering. *Chem. Mater.* **2015**, *27*, 3341–3348.

(15) Jiang, J.; Walters, D. M.; Zhou, D.; Ediger, M. D. Substrate Temperature Controls Molecular Orientation in Two-Component Vapor-Deposited Glasses. *Soft Matter* **2016**, *12*, 3265–3270.

(16) Yokoyama, D.; Setoguchi, Y.; Sakaguchi, A.; Suzuki, M.; Adachi, C. Orientation Control of Linear-Shaped Molecules in Vacuum-Deposited Organic Amorphous Films and Its Effect on Carrier Mobilities. *Adv. Funct. Mater.* **2010**, *20*, 386–391.

(17) Kato, T.; Mori, T.; Mizutani, T. Effect of Fabrication Conditions on Photoluminescence and Absorption of Hole Transport Materials. *Thin Solid Films* **2001**, *393*, 109–113.

(18) Sakai, Y.; Shibata, M.; Yokoyama, D. Simple Model-Free Estimation of Orientation Order Parameters of Vacuum-Deposited and Spin-Coated Amorphous Films Used in Organic Light-Emitting Diodes. *Appl. Phys. Express* **2015**, *8*, 096601.

(19) Lin, H.-W.; Lin, C.-L.; Chang, H.-H.; Lin, Y.-T.; Wu, C.-C.; Chen, Y.-M.; Chen, R.-T.; Chien, Y.-Y.; Wong, K.-T. Anisotropic Optical Properties and Molecular Orientation in Vacuum-Deposited ter(9,9-Diarylfluorene)s Thin Films Using Spectroscopic Ellipsometry. *J. Appl. Phys.* **2004**, *95*, 881–886.

(20) Yokoyama, D. Molecular Orientation in Small-Molecule Organic Light-Emitting Diodes. *J. Mater. Chem.* **2011**, *21*, 19187–19202.

(21) Shibata, M.; Sakai, Y.; Yokoyama, D. Advantages and Disadvantages of Vacuum-Deposited and Spin-Coated Amorphous Organic Semiconductor Films for Organic Light-Emitting Diodes. *J. Mater. Chem. C* **2015**, *3*, 11178–11191.

(22) Chen, W.; Huang, H.; Chen, S.; Huang, Y. L.; Gao, X. Y.; Wee, A. T. S. Molecular Orientation-Dependent Ionization Potential of Organic Thin Films. *Chem. Mater.* **2008**, *20*, 7017–7021.

(23) Scott, J. C.; Malliaras, G. G. Charge Injection and Recombination at the Metal–Organic Interface. *Chem. Phys. Lett.* **1999**, *299*, 115–119.

(24) Wang, Z. B.; Helander, M. G.; Greiner, M. T.; Qiu, J.; Lu, Z. H. Analysis of Charge-Injection Characteristics at Electrode-Organic Interfaces: Case Study of Transition-Metal Oxides. *Phys. Rev. B* **2009**, *80*, 235325.

(25) Wang, Z. B.; Helander, M. G.; Greiner, M. T.; Qiu, J.; Lu, Z. H. Carrier Mobility of Organic Semiconductors Based on Current-Voltage Characteristics. *J. Appl. Phys.* **2010**, *107*, 034506.

(26) Liew, Y.-F.; Aziz, H.; Hu, N.-X.; Chan, H. S.-O.; Xu, G.; Popovic, Z. Investigation of the Sites of Dark Spots in Organic Light-Emitting Devices. *Appl. Phys. Lett.* **2000**, *77*, 2650–2652.

(27) Kondakov, D. Y. Role of Chemical Reactions of Arylamine Hole Transport Materials in Operational Degradation of Organic Light-Emitting Diodes. *J. Appl. Phys.* **2008**, *104*, 084520.

(28) Torres, J. M.; Bakken, N.; Li, J.; Vogt, B. D. Substrate Temperature to Control Moduli and Water Uptake in Thin Films of Vapor Deposited *N,N*′-Di(1-Naphthyl)- *N,N*′-Diphenyl-(1,1′-Biphenyl)-4,4′-Diamine (NPD). *J. Phys. Chem. B* **2015**, *119*, 11928–11934.

(29) Brütting, W.; Frischeisen, J.; Schmidt, T. D.; Scholz, B. J.; Mayr, C. Device Efficiency of Organic Light-Emitting Diodes: Progress by Improved Light Outcoupling. *Phys. Status Solidi Appl. Mater. Sci.* **2013**, *210*, 44–65.

(30) Komino, T.; Tanaka, H.; Adachi, C. Selectively Controlled Orientational Order in Linear-Shaped Thermally Activated Delayed Fluorescent Dopants. *Chem. Mater.* **2014**, *26*, 3665–3671.

(31) Xiang, H.-F.; Xu, Z.-X.; Roy, V. A. L.; Che, C.-M.; Lai, P. T. Method for Measurement of the Density of Thin Films of Small Organic Molecules. *Rev. Sci. Instrum.* **2007**, *78*, 034104.